

## Influence of the Cation Distribution on the Magnetization of Y-type Hexagonal Ferrites

G. Albanese, M. Carbucicchio, and A. Deriu

Istituto di Fisica dell'Università di Parma, Italy

G. Asti and S. Rinaldi

Laboratorio MASPEC del CNR, Parma, Italy

Received 17 December 1974/Accepted 4 March 1975

**Abstract.** Mössbauer absorption and magnetization measurements have been made in  $Mg_2$ -Y and  $Co_2$ -Y ferrites. The magnetizations of the various iron sublattices did not show any marked difference in  $Mg_2$ -Y, whilst in the case of  $Co_2$ -Y three different behaviours of the sublattice magnetizations have been detected.

Low-temperature magnetization measurements in  $Mg_2$ Y gave evidence of a non-collinear magnetic order. The different magnetic properties of these compounds have been explained on the ground of a preferential occupation by  $Mg^{2+}$  and  $Co^{2+}$  ions of the inner octahedral sites of the T crystallographic block. The presence in these sites of a non-magnetic ion such as  $Mg^{2+}$  is responsible for the peculiar magnetic order observed in  $Mg_2$ -Y.

**Index Headings:** Hexagonal ferrites – Magnetization processes – Magnetic structures

A great interest has been devoted in recent years to hexagonal ferrites of various types (M, Y, Z) both as non-substituted and as substituted compounds.

The hexagonal ferrites are characterized by the complexity and dimensions of their unitary cells [1], as compared to those of other magnetic oxides. Moreover, some of their properties are mainly due to the presence of lattice sites having peculiar symmetry, such as the well known 2b site of M-type ferrites. The resulting magnetic structures are likely to show marked deviations from the usual magnetic order of the simple ferrimagnets and in general give rise to unusual magnetic properties, especially as it regards the magnetic anisotropy. As a matter of fact helical spin order and block structures have already been observed in several compounds of the M, Y, and Z types [2–4].

The problem of a better understanding of the magnetic properties of these materials is still open particularly

in what concerns the fundamental interactions responsible for the magnetic behaviour at different temperatures and in the presence of external magnetic fields. The magnetic superstructures observed in these compounds are usually rather regular despite the fact that in most cases they occur in compounds where Fe ions are partly substituted by non-magnetic ions. In other ferrimagnetic oxides such as the garnets, the substitution is considered, in general, not to induce magnetic superstructures but to give rise to disorder effects generally referred as the random canting [5], or random flip [6].

Until now the only hexagonal ferrites which were believed to exhibit unusual magnetic structures were some substituted M, and some Y and Z type ferrites containing Sr as divalent large cation. As opposed to this, we found non-collinear magnetic order in a non-substituted Y compound not containing Sr, namely  $Ba_2Mg_2Fe_{12}O_{22}$  ( $Mg_2$ Y). In fact, the magnetization

curves we have measured show a magnetic order transition very similar to the one reported by Enz [7] in  $(\text{BaSr})_2\text{Zn}_2\text{Fe}_{12}\text{O}_{22}$  compounds and by Perekalina *et al.* [8], in  $\text{Sr}_2\text{Zn}_2\text{Y}$  and  $\text{Sr}_3\text{Zn}_2\text{Z}$ .

Our analysis has been extended to  $\text{Ba}_2\text{Co}_2\text{Fe}_{12}\text{O}_{22}$  ( $\text{Co}_2\text{Y}$ ), an Y ferrite containing a divalent cation  $\text{Co}^{2+}$ , having a marked preference for octahedral sites just like  $\text{Mg}^{2+}$ , but carrying a magnetic moment. A comparative analysis of the magnetic properties of  $\text{Mg}_2\text{Y}$  and  $\text{Co}_2\text{Y}$  compounds allows in principle to clarify the leading role of octahedral sites in determining the magnetic order of these ferrites. It seems indeed that the presence of a non-magnetic ion in the central octahedral sites of the T-block is responsible for a strong perturbation on the magnetic structure of the crystal; indeed these octahedral sites are nodal-like points in the network of the superexchange interactions. Besides the magnetic measurements, a detailed Mössbauer analysis was also carried out in order to gain informations on the properties of the different magnetic sublattices of these compounds. The obtained results are coherent and substantially confirm the correctness of the above mentioned considerations.

### 1. The Properties of the Y Structures

The Y compound  $\text{Ba}_2\text{Me}_2\text{Fe}_{12}\text{O}_{22}$  ( $\text{Me} = \text{Zn}, \text{Co}, \text{Mg}, \text{Mn}$  etc.) has crystal symmetry characterized by the space group  $R\bar{3}m$ . Its structure may be described in terms of an hexagonal elementary cell including 18 oxygen layers. This structure is built up by the superposition of spinel blocks (S) and the so called T blocks (Fig. 1). The unit cell is composed by the sequence STSTST including three formula unit  $\text{Ba}_2\text{Me}_2\text{Fe}_{12}\text{O}_{22}$ . The T-block is typical of the Y structure and is formed by four oxygen layers with hexagonal packing; the two inner layers contain three oxygen ions and one barium ion. There are only two kinds of interstitial sites available for the metallic ions, namely six octahedral and two tetrahedral sites. Three octahedral sites are shared with the adjacent spinel blocks, while the other three lie on a vertical threefold axis, the central one having two faces of its coordination figure shared with the two adjacent sites. As we shall see, this peculiar aspect of the coordination figures of the inner octahedral sites of the T block plays an important role in determining the cation distribution of Y compounds.

In Table 1 we report the various metallic lattice sites together with their coordination and spin orientation

Table 1. Number of ions, coordination and spin orientation for the various metallic sublattices of Y structure

Sublattice	Coordination	Block	Number of ions per unit cell	Spin
$6c_{\text{IV}}$	tetrahedral	S	6	down
$3a_{\text{VI}}$	octahedral	S	3	up
$18h_{\text{VI}}$	octahedral	S-T	18	up
$6c_{\text{VI}}$	octahedral	T	6	down
$6c_{\text{IV}}^*$	tetrahedral	T	6	down
$3b_{\text{VI}}$	octahedral	T	3	up

which follow the scheme indicated by Gorter [9]. The nomenclature assigned to the different sublattices corresponds to the standard crystallographic notations (Wyckoff notations).

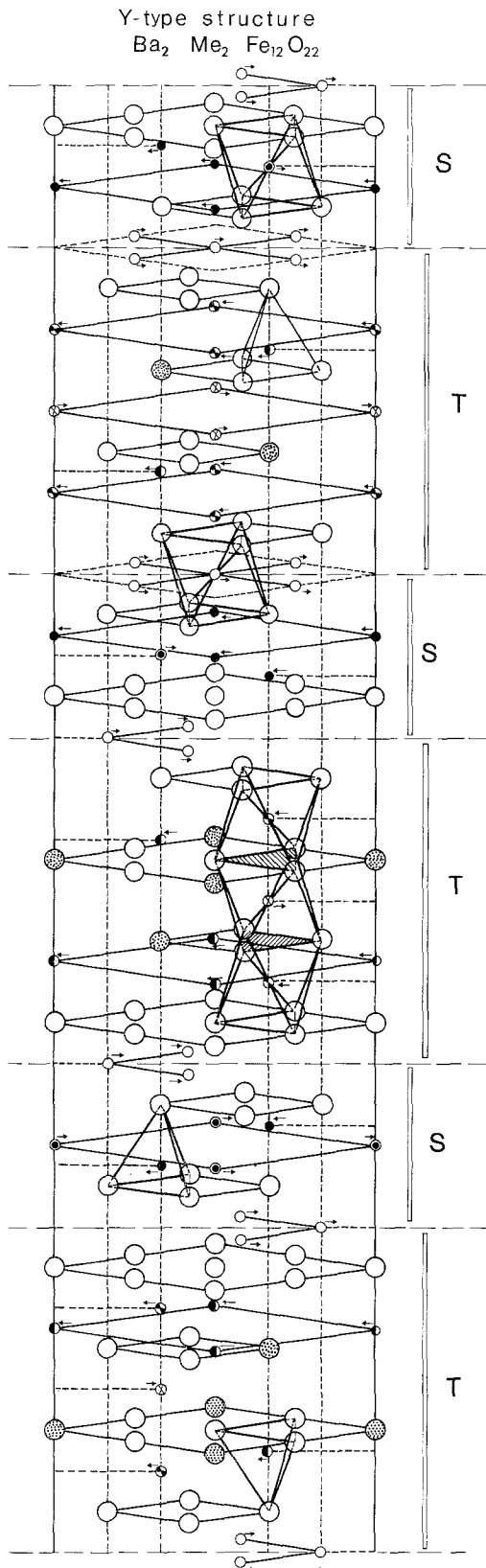
In Fig. 1 the different lattice sites are distinguished by different symbols; the spin orientation and the coordination figures of all the interstitial cations are also evidenced; the common faces of the octahedra inside the T block are hatched.

The presence of anion octahedra with common faces is generally responsible for a lower stability of the structure due to an higher potential energy of the system as compared, for instance, with situations where only corners are shared and the cations are then farther apart. This fact favours the entrance in the corresponding cation sites of ions having lower valency [10]. Thus when the  $\text{Me}^{2+}$  ions have a marked preference for octahedral coordination, we reasonably expect that they are mostly located in  $6c_{\text{VI}}$  and  $3b_{\text{VI}}$  lattice sites.

In order to account for the equilibrium magnetic order, and to evaluate the possible effects of localized strong perturbations, like those caused by the presence of non-magnetic ions in interstitial lattice sites, it is important to consider both the configuration of the chains of superexchange interactions and their relative strength. For this reason we have computed the Fe–O distances and the angles of Fe–O–Fe bonds assuming for the coordinates of the ions the values given by Brown [11], for the  $\text{Zn}_2\text{Y}$  compound.

From these data the strength of the interactions has been calculated according to a simple model in which we assume that the interaction energy  $E$  follows an exponential dependence on the anion-cation distances and a  $\cos^2\theta$  law for the angular dependence.

Table 2 reports the results obtained for the various interactions.



Although the adopted model can be considered quite approximated and the exact values of ions coordinates slightly depend upon the kind of divalent cations present in the structure, we assume that the obtained values of the interaction strengths are at least indicative of the effective role played by the various interactions in the Y-structure. From Table 2 it appears that the strongest superexchange interaction is the one between the tetrahedral ions  $6c_{IV}^*$  and the octahedral ions  $3b_{VI}$  inside the T block; moreover the only appreciable perturbing interaction appears to be the one between  $6c_{IV}^*$  and  $6c_{VI}$  ions, both belonging to the T block.

As we noticed before, in the hexagonal ferrites the structure of the chains of superexchange interactions is rather complex and in particular there are lattice sites which play a very important role in determining the magnetic order due to the fact that they are nodal-like points. This fact, together with the large dimensions of the unit cell characteristic of the hexagonal ferrites, justifies the occurrence of block magnetic structures where the collinear order inside the blocks coexists with the angular order between them [2-4]. This phenomenon can occur either when part of the interstitial lattice sites are occupied by non-magnetic ions or when localized lattice distortions and symmetry breaking are induced by the simultaneous presence in the oxygen planes of ions having different ionic radius such as Sr and Ba. In the Y structure one can reasonably expect that the entrance of a non-magnetic ion in  $3b_{VI}$  sites might cause a drastic change in the magnetic order. In fact this site alone links the upper and lower part of the unit cell through the strong interaction with six ions  $6c_{IV}^*$ . Furthermore, the partial substitution of iron ions in  $6c_{VI}$  sites results in the breaking of the inversion symmetry around  $3b_{VI}$  sites. As a consequence antisymmetric interactions between couples of ions on opposite sides of  $3b_{VI}$  sites, like  $6c_{VI}$  or  $18h_{VI}$  ions, are allowed. In this case according to the fifth Moriya rule [12], the antisymmetric exchange vector  $\mathbf{D}$  must be parallel to the  $c$ -axis thus favouring the formation of angles between the moments lying in the basal plane.

Fig. 1. Unit cell of the Ba<sub>2</sub>Me<sub>2</sub>Fe<sub>12</sub>O<sub>22</sub> (Me<sub>2</sub>Y) ferrite. The anions O<sup>2-</sup> (large empty circles), the divalent barium cations Ba<sup>2+</sup> (large dotted circles), the metallic ions in the sublattices  $3a_{VI}$  (●),  $6c_{VI}$  (⊙),  $3b_{VI}$  (⊗),  $18h_{VI}$  (○),  $6c_{IV}$  (●) and  $6c_{IV}^*$  (●) are indicated. The coordination figures of the metallic ions in the different lattice sites, together with their spin orientation, are put in evidence

Table 2. Strength of the superexchange interactions between  $\text{Fe}^{3+}$  ions in the Y structure

Each $\text{Fe}^{3+}$ ion in lattice position	Interacts with $n$ $\text{Fe}^{3+}$ ions		Strength of the superexchange interaction [K] <sup>a</sup>
	$n$	lattice position	
$3a_{\text{VI}}$	6	$6c_{\text{IV}}$	25
	6	$18h_{\text{VI}}$	0(+)
$6c_{\text{IV}}$	3	$6c_{\text{IV}}$	0(+)
	3	$3a_{\text{VI}}$	25
	9	$18h_{\text{VI}}$	26
$18h_{\text{VI}}$	1	$3a_{\text{VI}}$	0(+)
	3	$6c_{\text{IV}}$	26
	2	$6c_{\text{VI}}$	30
	1	$6c_{\text{IV}}^*$	25
	4	$18h_{\text{VI}}$	0(+)
$6c_{\text{VI}}$	6	$18h_{\text{VI}}$	30
	3	$6c_{\text{IV}}^*$	9(+)
	1	$3b_{\text{VI}}$	1.7
$6c_{\text{IV}}^*$	3	$6c_{\text{VI}}$	9(+)
	3	$18h_{\text{VI}}$	25
	3	$3b_{\text{VI}}$	77
$3b_{\text{VI}}$	6	$6c_{\text{IV}}^*$	77
	2	$6c_{\text{VI}}$	1.7

<sup>a</sup> The cross indicates interactions between sublattices with parallel spins.

## 2. Experimental Procedure

The compound  $\text{Mg}_2\text{Y}$  was supplied by Harshaw Chem. Co. in form of small single crystals grown by the flux method. The sample of  $\text{Co}_2\text{Y}$  has been prepared as sintered polycrystals in the chemistry division of Maspec Laboratory. All the samples we have examined have been checked both by X-ray diffraction from oriented powders and by chemical analysis. Moreover, in order to better ascertain the homogeneity of the samples, we have carried out measurements of the saturation magnetization and of the Mössbauer absorption as a function of temperature near the Curie temperature. The data have clearly shown a single, well defined, Curie temperature, thus confirming the absence of extraneous phases.

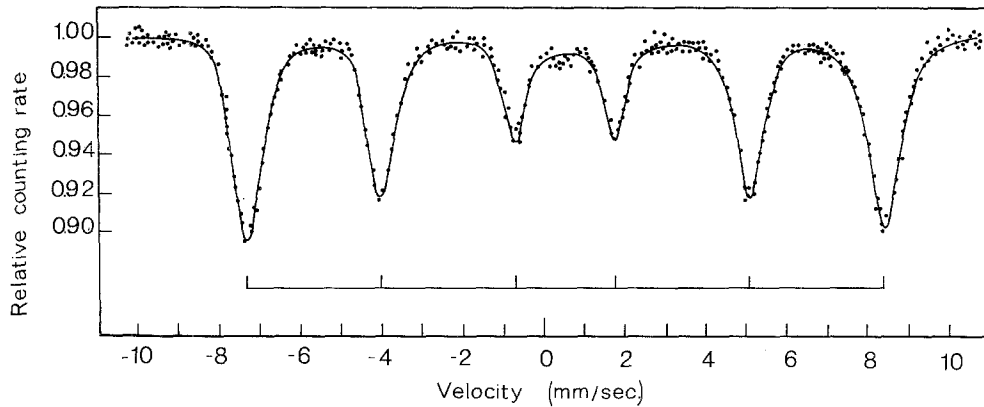
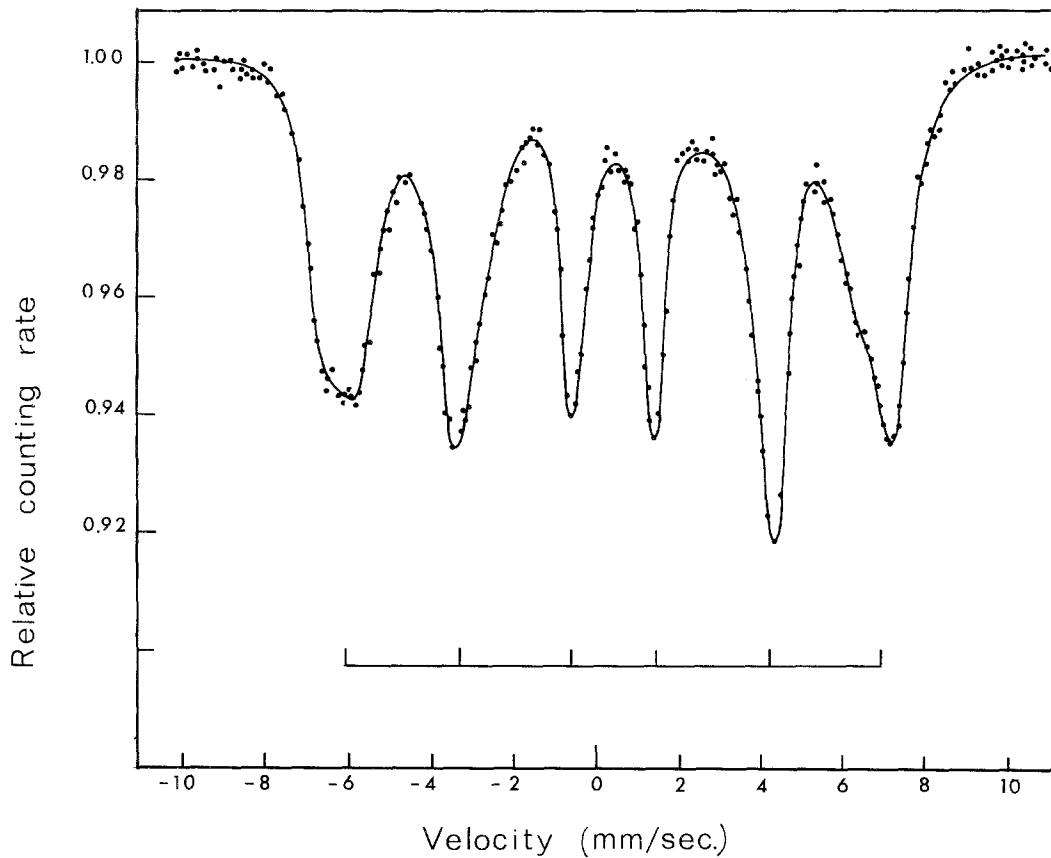
The Mössbauer absorption spectra have been measured by means of a standard spectrometer consisting of a constant acceleration electromechanical driving system and a multichannel analyser working in multiscaler time mode. The source employed was a 10 mC  $\text{Co}^{57}$  in Cr matrix while the absorbers of  $\text{Mg}_2\text{Y}$  and  $\text{Co}_2\text{Y}$  were prepared by grinding the samples previously selected. The spectra have been measured with the source at room temperature and the absorber maintained at different temperatures in the range from 78 to 700 K.

The magnetization measurements have been carried out by means of a vibrating sample magnetometer equipped with cryostat and oven assembly only for  $\text{Mg}_2\text{Y}$  single crystals, while for  $\text{Co}_2\text{Y}$  we have taken the data reported in the literature which refer to single crystals.

## 3. Experimental Results and Discussion

### $\text{Mg}_2\text{Y}$ Compound

The Mössbauer absorption spectra of the  $\text{Fe}^{57}$  14.4 keV gamma rays measured for polycrystalline  $\text{Mg}_2\text{Y}$  samples at 78 and 300 K are shown in Figs. 2 and 3, respectively. The spectrum at 78 K shows only one Zeeman sextet ( $H_{hf} = 484$  KOe). With increasing temperature the lines become broader showing that the magnetizations of the various sublattices have a slightly different temperature dependence. However, it is not possible to resolve more than one sextet. Therefore we evaluate a mean value of the hyperfine field from the center of the lines. The observed line widths imply that the hyperfine fields relative to the various iron sublattices deviate from the mean value by less than 15 KOe. The fact that the hyperfine fields relative to the various sublattices have nearly the same intensity, appears to be common to all the Y com-

Fig. 2. Mössbauer spectrum for  $Mg_2Y$  compound at  $T = 78$  KFig. 3. Mössbauer spectrum for  $Mg_2Y$  compound at  $T = 300$  K

pounds. It can be related to the absence in Y structure of the R block which is instead present in the other hexagonal structures, viz. M, W, Z etc. Indeed it is known that both the perturbing interactions arising from iron ions located in the bipyramidal lattice sites

of the R block and the intrasublattice interactions give rise to a marked reduction in the magnetization of 12 K sublattice [9, 14].

Figure 4 reports the reduced values of the mean hyperfine field  $H_{hf}(T)/H_{hf}(O)$  as a function of temperature

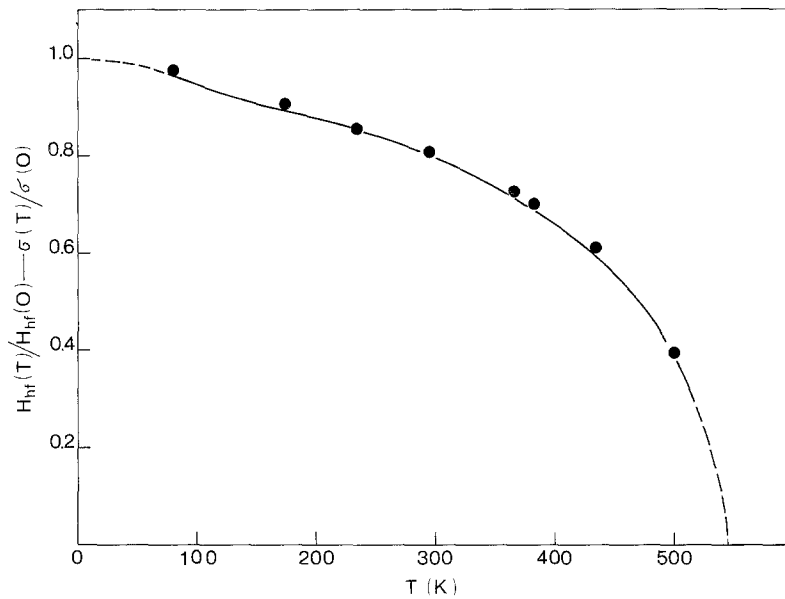


Fig. 4. Temperature dependence of the reduced values of the mean hyperfine field  $H_{hf}(T)/H_{hf}(0)$  (full circles) and of the magnetization  $\sigma(T)/\sigma(0)$  (solid line) for the compound  $Mg_2Y$

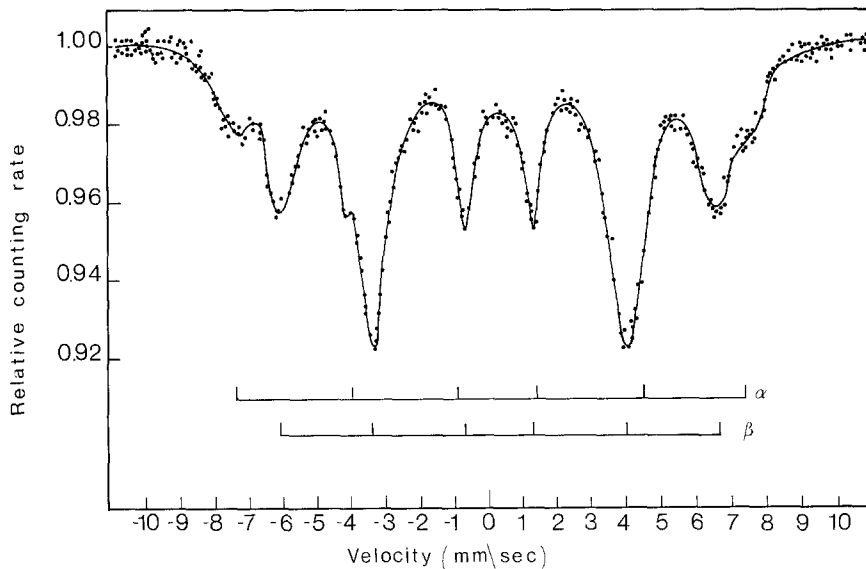


Fig. 5. Mössbauer spectrum for  $Mg_2Y$  compound at room temperature in an external magnetic field of 25 KOe

for the  $Mg_2Y$  ferrite. The Curie temperature has been determined by measuring the line-width of the absorption spectrum near the Curie point as a function of  $T$ . The obtained value for  $Mg_2Y$  is  $T_c = 275 \pm 5^\circ C$  in agreement with published data [1]. In order to evaluate the distribution of  $Fe^{3+}$  ions between the spin-up and spin-down sublattices, we have measured absorption spectra keeping the absorber at room tem-

perature in an external magnetic field of 25 KOe. As it is evident from the spectrum reported in Fig. 5, the room temperature single Zeeman sextet with an hyperfine field of  $415 \pm 15$  KOe splits into two well defined sextets  $\alpha$  and  $\beta$  with hyperfine fields of  $450 \pm 10$  KOe and  $390 \pm 10$  KOe, respectively. Due to the fact that the hyperfine field is opposite to the atomic magnetic moments, the dominant sublattice

corresponds to the  $\beta$  sextet, i.e. the one with the lower hyperfine field, while the  $\alpha$  sextet corresponds to all the  $\text{Fe}^{3+}$  ions with spin down.

We have also measured the magnetization curves of single crystal samples at different temperatures for various crystallographic orientations. The easy directions have been verified to lie in the basal plane. The reduced magnetization  $\sigma(T)/\sigma(0)$  measured in easy direction in an external field of 20 KOe as function of temperature is reported in Fig. 4. The Curie temperature turns out to be  $280 \pm 5^\circ \text{C}$ , in agreement with the above reported value obtained from Mössbauer measurements. We have evaluated by extrapolation to 0 K the values of the saturation magnetization  $\sigma_0$ , which turns out to be 29 Gauss  $\text{cm}^3/\text{g}$  in agreement with previously reported values [1].

Assuming for the atomic magnetic moment of  $\text{Fe}^{3+}$  ions the value of  $5 \mu_B$  and the usual magnetic order attributed to the Y-structure, we have determined from the obtained value of  $\sigma_0$  the distribution of  $\text{Mg}^{2+}$  ions between up and down sublattices; it turns out that 1.3  $\text{Mg}^{2+}$  ions per unit formula occupy sites belonging to the spin-up sublattice, and 0.7 enter the spin-down sublattice.

As it regards the distribution of  $\text{Mg}^{2+}$  among the octahedral spin-up sites we expect a marked preference for  $3b_{\text{VI}}$  sites for the reasons explained in Section 1 concerning the coordination figures with common faces. Moreover, taking into account that  $\text{Mg}^{2+}$  ions have a marked preference for the octahedral coordination, we expect that most of the 0.7  $\text{Mg}^{2+}$  ions in the spin-down sublattice occupy the  $6c_{\text{VI}}$  sites, which also share a face of their coordination figures with  $3b_{\text{VI}}$  ions. This cation distribution is in agreement with the one deducible from the relative intensities of the two sextets  $\alpha$  and  $\beta$  of the spectrum measured in external field.

The temperature dependence of the reduced values of the mean hyperfine field  $H_{\text{hf}}(T)/H_{\text{hf}}(0)$  is compared in Fig. 4 with the temperature dependence of the reduced magnetization  $\sigma(T)/\sigma(0)$ . As it is evident, the two dependences are substantially the same.

We have also measured at different temperatures the dependence of the magnetization  $\sigma$  on the applied field both along the  $c$ -axis and in the basal plane. We have thus verified that  $\text{Mg}_2\text{Y}$  has a planar anisotropy as it appears from the magnetization curve reported in Fig. 6. Since the anisotropy field is rather high, it is necessary to apply a field of 20 KOe in order to achieve saturation: the values of  $\sigma(T)$  reported in Figs. 4 and 7 are the values obtained with  $H_{\text{ext}}$

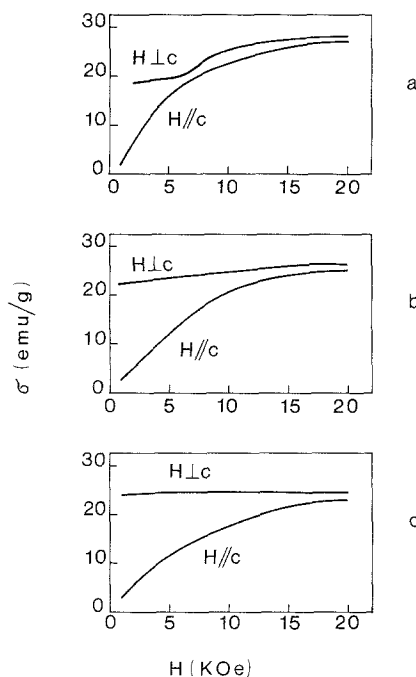


Fig. 6a—c. Magnetization curves for  $\text{Mg}_2\text{Y}$  single crystal at (a)  $T = 90 \text{ K}$ , (b)  $T = 150 \text{ K}$ , and (c)  $T = 250 \text{ K}$

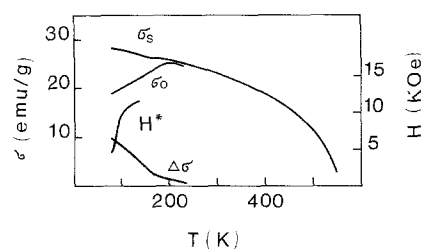


Fig. 7. Temperature dependence of the saturation magnetization at 20 KOe ( $\sigma_s$ ), of the spontaneous magnetization ( $\sigma_0$ ), of the difference  $\Delta\sigma = \sigma_s - \sigma_0$  and of the critical field ( $H^*$ ) where the differential susceptibility shows an abrupt increase, for  $\text{Mg}_2\text{Y}$  single crystal

$= 20 \text{ KOe}$ . With decreasing temperature one notices an appreciable differential susceptibility which is nearly constant from 2 to 10 KOe in the curve with  $H_{\text{ext}}$  perpendicular to the  $c$ -axis.

A rather peculiar effect is observed at even lower temperatures (Fig. 6); a knee appears in the easy magnetization curve at a critical field  $H^*$ , having a magnitude of some KOe. At this field the magnetization curve exhibits a sharp increase in slope and reaches saturation at an higher field.

We have plotted (Fig. 7) the temperature dependence of various parameters which characterize the shape of

the magnetization curve, namely:

$\sigma_s$  = the magnetization measured at 20 KOe,

$\sigma_0$  = the extrapolated value of  $\sigma$  at  $H = 0$ ,

$\Delta\sigma = \sigma_s - \sigma_0$ ,

$H^*$  = the critical field where the differential susceptibility shows an abrupt increase.

As it is evident the magnetization  $\sigma_s$  shows an inflection point at  $T \simeq 175$  K which is near to the temperature where the knee in the magnetization curve appears. The spontaneous magnetization at zero field  $\sigma_0$  and the critical field  $H^*$  decrease with decreasing temperature. A similar behaviour of the magnetization curves has already been observed in  $(\text{Ba}_{1-x}\text{Sr}_x)_2\text{Zn}_2\text{Fe}_{12}\text{O}_{22}$  and  $(\text{Ba}_{1-x}\text{Sr}_x)_2\text{Zn}_2\text{Fe}_{24}\text{O}_{41}$  [8]. The present case, however, is the first for an hexagonal ferrite not containing Sr. The observed anomalies in the magnetization curve of the  $\text{Mg}_2\text{Y}$  ferrite can be interpreted in the light of the general considerations made in Section 1 taking into account that the preferential occupation both of  $3b_{\text{VI}}$  and  $6c_{\text{VI}}$  sites by  $\text{Mg}^{2+}$  ions leads to a critical competition of the two exchange interactions  $3b_{\text{VI}} - 6c_{\text{IV}}^*$  and  $6c_{\text{VI}} - 6c_{\text{IV}}^*$ ; consequently antisymmetric exchange interactions although weak may become important. As a consequence a formation of angles between the magnetic moments of structurally equivalent blocks can occur while inside each block the moments are collinearly ordered. The resulting magnetic structure can be similar to the "quasi-helical" or "block flat spiral structure" described by Sizov *et al.* for the case of  $(\text{Sr}_{1-x}\text{Ba}_x)_2\text{Zn}_2\text{Fe}_{12}\text{O}_{22}$  compounds [3]. The magnetic behaviour of this kind of materials having magnetic block structures can be probably described on the basis of a two sublattice model having uniaxial anisotropy and a Dzialoshinsky-Moriya (D.M.) exchange interaction. In fact recent models [13, 15, 16] developed for two sublattice systems described by an Hamiltonian containing isotropic exchange, uniaxial anisotropy and D.M. interaction terms indicate that different canted states and second-order spin-flop transitions are possible. In these cases the magnetization curves, at various temperatures, can display features similar to those we have observed in  $\text{Mg}_2\text{Y}$ .

### $\text{Co}_2\text{Y}$ Compound

The Mössbauer absorption spectra of  $\text{Fe}^{57}$  14.4 keV  $\gamma$ -rays for polycrystalline samples of  $\text{Co}_2\text{Y}$  at different temperatures are shown in Fig. 8. The spectrum measured at 78 K shows only one Zeeman sextet with a mean hyperfine magnetic field of 508 KOe.

With increasing temperature the obtained spectra can be interpreted as the superposition of several sextets. However, the separation of the different sextets contributing to the spectra is not straightforward. A satisfactory fit of the spectrum is possible only if we superimpose at least three different sextets. Thus, with an uncertainty of  $\pm 10$  KOe in the values of hyperfine fields, we have distinguished the sextets I, II, and III shown in Fig. 8. This interpretation is also supported by the spectrum measured with the sample at room temperature in an external field of 25 KOe perpendicular to the  $\gamma$ -rays direction (Fig. 9). The spectrum can be analyzed in two sextets  $\alpha$  and  $\beta$  having hyperfine fields of  $(490 \pm 10)$  and  $(425 \pm 10)$  KOe, respectively. In fact, sextet  $\beta$  appears to be the superposition of sextets I and II while  $\alpha$  may be identified with sextet III. Sextets I and III are expanded by an amount corresponding to the intensity of the external field thus indicating that they are due to  $\text{Fe}^{3+}$  ions with spin down. Sextet II instead is contracted by the same amount and is then due to  $\text{Fe}^{3+}$  ions in spin up sublattices. This interpretation is consistent with the intensity analysis of the spectra at room temperature with and without external field. Figure 10 reports the temperature dependence of the hyperfine magnetic fields relative to sextets I, II, and III.

We have also measured the Curie temperature following the same procedure described for  $\text{Mg}_2\text{Y}$  obtaining  $T_c = (340 \pm 5)^\circ\text{C}$ , in agreement with published data [1]. The spectrum measured at  $T > T_c$  (Fig. 8d) shows an absorption peak having a half-height width  $\Gamma = 0.93$  mm/sec. As for the case of  $\text{Mg}_2\text{Y}$  we determined the distribution of  $\text{Co}^{2+}$  from the saturation magnetization  $\sigma_0$  at 0 K. If we utilize the value reported in the literature [1],  $\sigma_0 = 39$  Gauss  $\text{cm}^3/\text{g}$  which corresponds to  $9.8 \mu_B$  per unit formula, and assign a moment of  $3.7 \mu_B$  to  $\text{Co}^{2+}$  ions, we obtain that 1.1  $\text{Co}^{2+}$  ions per unit formula occupy spin up and 0.9 spin down lattice sites. Since  $\text{Co}^{2+}$  ions have a marked preference for octahedral coordination, 0.9 cobalt ions are located in the only spin down octahedral sublattice  $6c_{\text{VI}}$ ; whilst the remanent 1.1 are supposed to be distributed among  $3a_{\text{VI}}$ ,  $18h_{\text{VI}}$ ,  $3b_{\text{VI}}$  sublattices.

We can now try to establish the correspondence between the three observed sextets (Fig. 8) and the iron sublattices of  $\text{Co}_2\text{Y}$  structure. Sextet II, being the only one which is contracted in the presence of the external field, is due to all the  $\text{Fe}^{3+}$  ions with spin up, i.e. the sublattices  $18h_{\text{VI}}$ ,  $3a_{\text{VI}}$ ,  $3b_{\text{VI}}$ . Sextet III, the one having



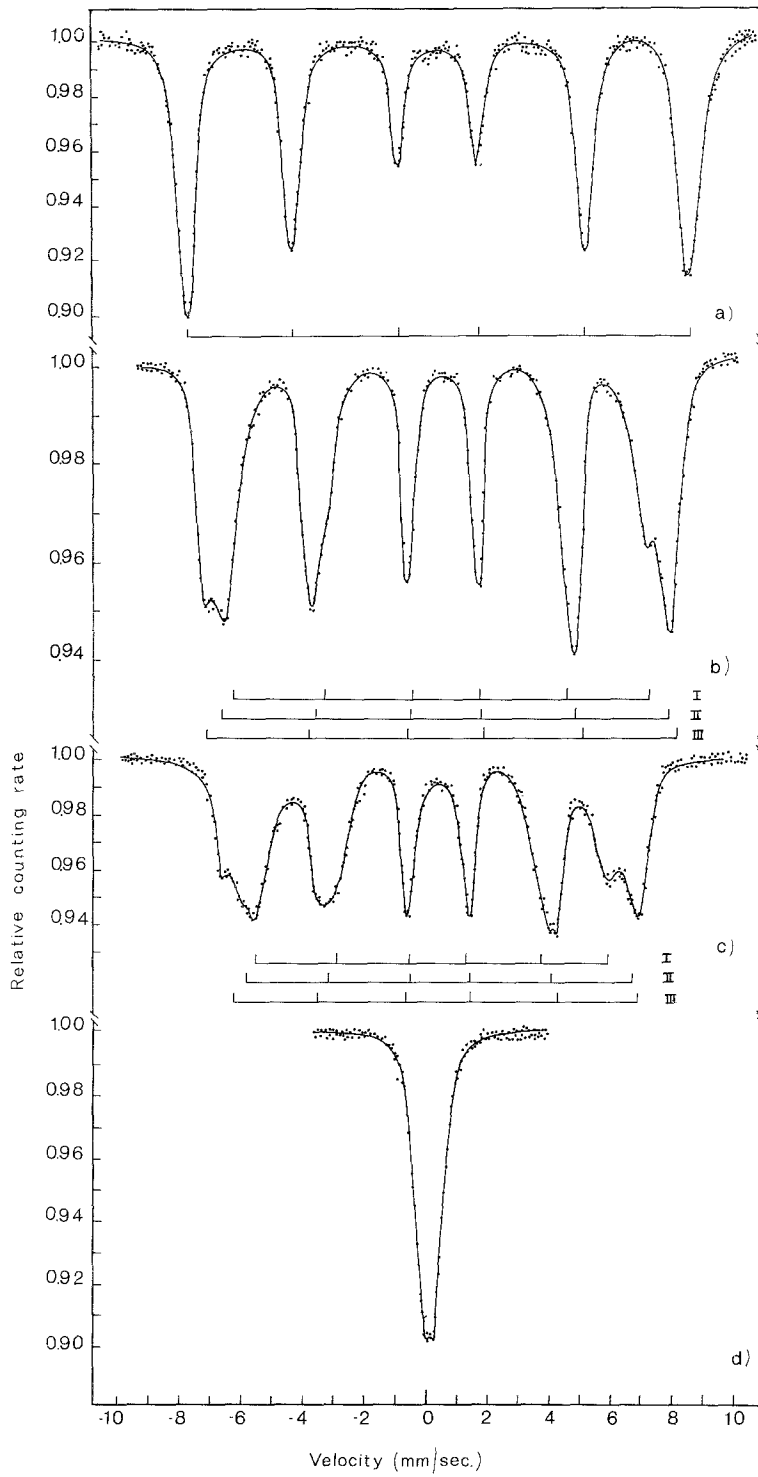


Fig. 8a—d. Mössbauer spectra for  $\text{Co}_2\text{Y}$  compound (a)  $T = 78 \text{ K}$ , (b)  $T = 296 \text{ K}$ , (c)  $T = 403 \text{ K}$ , (d)  $T = 673 \text{ K}$ .

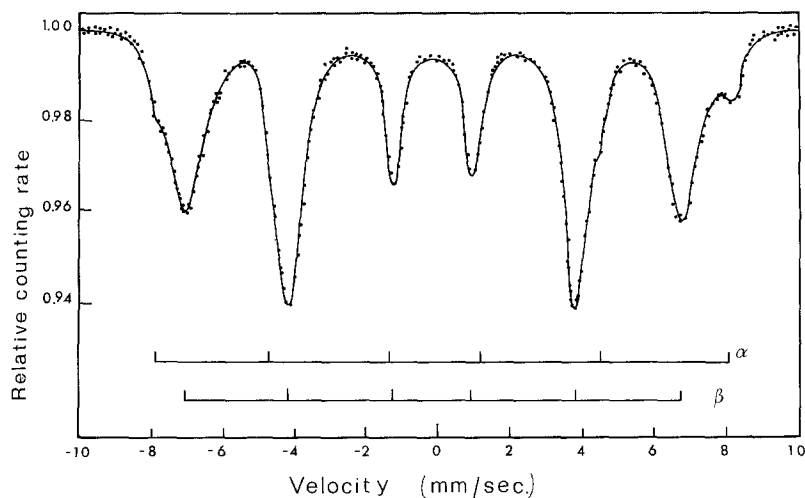


Fig. 9. Mössbauer spectrum for  $\text{Co}_2\text{Y}$  at room temperature in an external magnetic field of 25 KOe

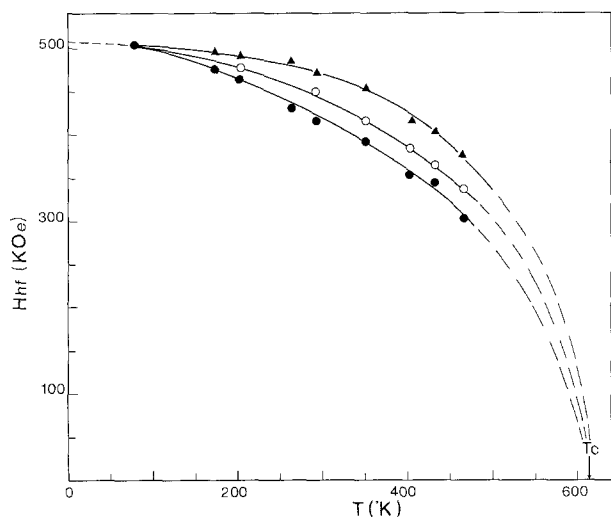


Fig. 10. Hyperfine magnetic fields at the  $\text{Fe}^{57}$  nuclei versus temperature for the various sublattices of  $\text{Co}_2\text{Y}$  compound. Full circles refer to sextet I, open circles refer to sextet II, full triangles refer to sextet III

the highest hyperfine field, can be assigned to the sublattice  $6c_{\text{IV}}^*$  on the ground of the spectrum taken in external field (Fig. 9). Indeed the area of the external line at positive velocity of  $\alpha$  sextet is about 0.2 of the corresponding line of  $\beta$  sextet. This indicates that sextet III must be assigned to a spin down sublattice containing two iron ions per unit formula i.e. either  $6c_{\text{IV}}^*$  or  $6c_{\text{IV}}$ . It seems reasonable to assign the sextet III to the sublattice  $6c_{\text{IV}}^*$  owing to the large positive superexchange interaction  $6c_{\text{IV}}^* - 3b_{\text{VI}}$  which may be responsible for the high hyperfine field of this sextet.

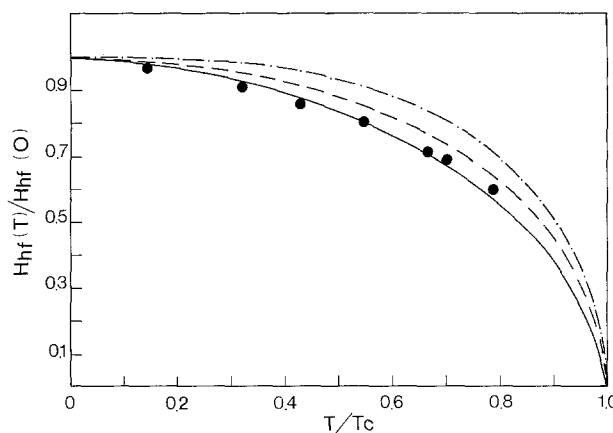


Fig. 11. Reduced values of the hyperfine fields versus reduced temperature for the compounds  $\text{Co}_2\text{Y}$  (sextet I —, sextet II ---, sextet III - · -) and  $\text{Mg}_2\text{Y}$  (solid circles)

At last, sextet I must be assigned to the remaining spin down sublattices i.e. to  $6c_{\text{IV}}$  and to the fraction of  $6c_{\text{VI}}$  sublattice occupied by iron ions.

The fact that the  $\text{Fe}^{3+}$  ions in  $6c_{\text{VI}}$  sublattice has the lowest moment is justified by taking into account the perturbing interaction with  $6c_{\text{IV}}^*$ , which is not negligible as one can see from Table 2.

This interpretation is confirmed from a comparison with the data obtained on  $\text{Mg}_2\text{Y}$ . In Fig. 11 we have plotted the dependence of the reduced values of hyperfine fields on the reduced temperature, for both  $\text{Co}_2\text{Y}$  and  $\text{Mg}_2\text{Y}$ . We observe that the temperature dependence of the mean hyperfine field measured for  $\text{Mg}_2\text{Y}$  is nearly the same as that relative to sextet I of  $\text{Co}_2\text{Y}$ , while the hyperfine fields relative to sextets II

and III lie well above. This fact can be explained as due to the weakening effects on the superexchange interactions caused by the presence of the non-magnetic ion  $\text{Mg}^{2+}$  mainly in  $6c_{\text{VI}}$  and  $3b_{\text{VI}}$  sublattices. Indeed as a consequence of the large occupation of  $3b_{\text{VI}}$  sites by  $\text{Mg}^{2+}$  ions the hyperfine field relative to the tetrahedral  $6c_{\text{IV}}^*$  sublattice is likely to be much smaller in  $\text{Mg}_2\text{Y}$  than in  $\text{Co}_2\text{Y}$ . Similar considerations are valid for sublattice  $18h_{\text{VI}}$  which gives the main contribution to sextet II, as far as the interaction  $18h_{\text{VI}}-6c_{\text{VI}}$  is concerned. On the contrary, the hyperfine field relative to  $6c_{\text{VI}}$  sublattice has the same behaviour in  $\text{Mg}_2\text{Y}$  and  $\text{Co}_2\text{Y}$ : indeed the strongest superexchange interaction orienting the moments of  $\text{Fe}^{3+}$  in  $6c_{\text{VI}}$  sites namely  $18h-6c_{\text{VI}}$ , does not change substantially going from  $\text{Co}_2\text{Y}$  to  $\text{Mg}_2\text{Y}$ , due to the fact that only a small fraction of  $18h_{\text{VI}}$  lattice sites is occupied by the divalent cations, i.e.  $\text{Co}^{2+}$  or  $\text{Mg}^{2+}$ .

In the frame of our interpretation of the Mössbauer spectra, by using the obtained hyperfine fields values at various temperatures, we have calculated the temperature dependence of the reduced magnetization  $\sigma/\sigma_0$  (Fig. 12) according to the formula

$$\sigma(T) = \alpha \sum_i (n_i - x_i) H_{h_f}^i(T) \mu_{\text{Fe}} + x_i H_{h_f}^i(T) \mu_{\text{Co}} \quad (2)$$

$$\alpha \sum_i (n_i - x_i) \mu_{\text{Fe}} + x_i \mu_{\text{Co}} H_{h_f}^i(T),$$

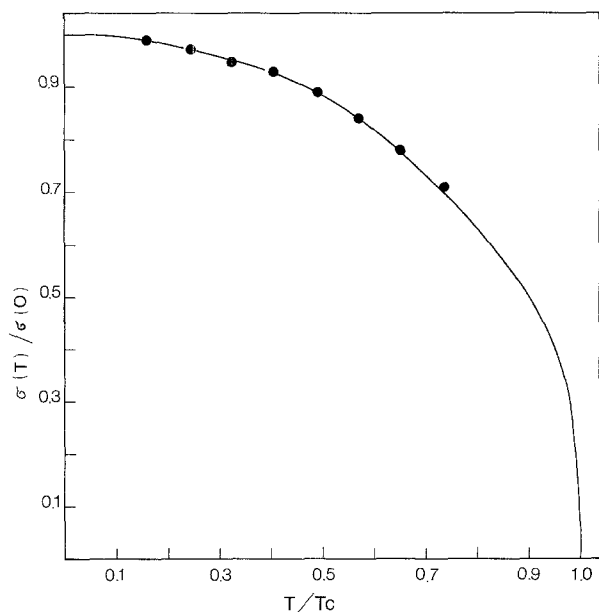


Fig. 12. Reduced values of the magnetization  $\sigma$  versus reduced temperature for the compound  $\text{Co}_2\text{Y}$ . The experimental values (solid line) and the calculated values (full circles) are reported

where  $\alpha$  is a constant independent on temperature,  $n_i$  is the number of metallic cations belonging to  $i$ -th sublattice per unit formula,  $x_i$  is the number of  $\text{Co}^{2+}$  ions in the  $i$ -th sublattice,  $\mu_{\text{Fe}}$  and  $\mu_{\text{Co}}$  are the atomic magnetic moments assigned to  $\text{Fe}^{3+}$  and  $\text{Co}^{2+}$  ions and  $H_{h_f}^i(T)$  is the hyperfine magnetic field relative to  $\text{Fe}^{3+}$  ions in  $i$ -th sublattice. As is clear from (2) we have attributed to the moment of  $\text{Co}^{2+}$  the same temperature dependence of the  $\text{Fe}^{3+}$  moment; this oversimplification is expected to have only negligible effects on the calculated  $\sigma(T)$ , because the  $\text{Co}^{2+}$  ions are nearly equally distributed between up and down sublattices. As it is evident from Fig. 12, the calculated curve  $\sigma(T)/\sigma_0$  is in agreement with the experimental one reported in the literature (1).

## Conclusions

Our measurements show that the magnetizations of the various sublattices of  $\text{Mg}_2\text{Y}$  have all the same temperature dependence, while for  $\text{Co}_2\text{Y}$  we distinguish three different behaviours of the sublattice magnetizations. For  $\text{Mg}_2\text{Y}$  a non-collinear magnetic order has been observed at low temperature.

These differences in the magnetic behaviour of these two materials are a consequence of the preferential occupation by the divalent cations  $\text{Mg}^{2+}$  and  $\text{Co}^{2+}$  of the octahedral sites inside the T block which are of primary importance in providing continuity in the chains of interactions. In particular the presence of a non-magnetic ion as  $\text{Mg}^{2+}$  in these sites is responsible for the formation of the magnetic block structure observed in  $\text{Mg}_2\text{Y}$  ferrite.

*Acknowledgements.* The authors wish to thank Dr. V. Fano who kindly supplied the  $\text{Co}_2\text{Y}$  sample, Dr. P. Ferretti for his collaboration in the Mössbauer measurements and Dr. M. Acquarone who performed the calculations of the strength of superexchange interactions.

## References

1. J. Smith, H. P. J. Wijn: *Ferrites* (Philips Technical Library, Eindhoven 1959)
2. M. I. Namtalishvili, O. P. Aleshko-Ozhevskii, I. I. Yamzin: *Soviet Phys.-Solid State* **13**, 2137 (1972)
3. V. A. Sizov, R. A. Sizov, I. I. Yamzin: *Soviet Phys. JETP* **26**, 736 (1968)
4. M. Namtalishvili, O. P. Aleshko-Ozhevskii, I. I. Yamzin: *Soviet Phys. JETP* **35**, 370 (1972)
5. A. Rosencwaig: *Canadian J. Phys.* **48**, 2857 (1970)  
S. Geller: *J. Appl. Phys.* **37**, 1408 (1966)

6. I. Nowik: *Phys. Rev.* **171**, 550 (1968); and *J. Appl. Phys.* **40**, 5184 (1969)
7. U. Enz: *J. Appl. Phys.* **32**, Suppl. 225 (1961)
8. T. M. Perekalina, A. D. Shchurova, S. S. Fonton, D. G. Sannikov: *Soviet Phys. JETP* **31**, 440 (1970)
9. E. W. Gorter: *Proc. IEE (London)*, **104B**, Suppl. No. 5, 255 (1957)
10. L. Pauling: *The Nature of the Chemical Bond* (Cornell University Press, Ithaca 1948)
11. P. G. Brown: *Philips Res. Repts.* **12**, 491 (1957)
12. T. Moriya: *Phys. Rev.* **120**, 91 (1960)
13. L. I. Koroleva, L. P. Mitina: *Phys. Stat. Sol. (a)* **5**, K 55 (1971)
14. G. Albanese, M. Carbucchio, A. Deriu: *Phys. Stat. Sol. (a)* **23**, 351 (1974)
15. B. R. Morrison: *Phys. Stat. Sol. (b)* **59**, 551 (1973)
16. N. Yamashita: *J. Phys. Soc. Japan* **32**, 610 (1972)

See also R. C. Evans: *Crystal Chemistry* (Cambridge University Press 1966)